doi:10.1016/j.jmb.2011.04.026 J. Mol. Biol. (2011) 410, 959–971

Contents lists available at www.sciencedirect.com

Journal of Molecular Biology

journal homepage: http://ees.elsevier.com.jmb

Single-Molecule Studies Reveal that DEAD Box Protein DDX1 Promotes Oligomerization of HIV-1 Rev on the Rev Response Element

Rae M. Robertson-Anderson, Jun Wang, Stephen P. Edgcomb, Andrew B. Carmel, James R. Williamson and David P. Millar*

Department of Molecular Biology, The Scripps Research Institute, 10550 North Torrey Pines Road, La Jolla, CA 92037, USA

Received 29 January 2011; received in revised form 10 April 2011; accepted 11 April 2011

Edited by M. F. Summers

Keywords:
viral RNA transport; cellular cofactors of HIV; ribonucleoprotein assembly; RNA–protein interactions; single-molecule fluorescence microscopy

Oligomeric assembly of Rev on the Rev response element (RRE) is essential for the nuclear export of unspliced and singly spliced human immunodeficiency virus type 1 viral mRNA transcripts. Several host factors, including the human DEAD box protein DDX1, are also known to be required for efficient Rev function. In this study, spontaneous assembly and dissociation of individual Rev–RRE complexes in the presence or absence of DDX1 were observed in real time via single-molecule total internal reflection fluorescence microscopy. Binding of up to eight fluorescently labeled Rev monomers to a single RRE molecule was visualized, and the event frequencies and corresponding binding and dissociation rates for the different Rev–RRE stoichiometries were determined. The presence of DDX1 eliminated a second kinetic phase present during the initial Rev binding step, attributed to nonproductive nucleation events, resulting in increased occurrence of higher-order Rev–RRE stoichiometries. This effect was further enhanced upon the addition of a non-hydrolyzable ATP analog (adenylyl-imidophosphate), whereas ADP had no effect beyond that of DDX1 alone. Notably, the first three Rev monomer binding events were accelerated in the presence of DDX1 and adenylyl-imidophosphate, while the dissociation rates remained unchanged. Measurements performed across a range of DDX1 concentrations suggest that DDX1 targets Rev rather than the RRE to promote oligomeric assembly. Moreover, DDX1 is able to restore the oligomerization activity of a Rev mutant that is otherwise unable to assemble on the RRE beyond a monomeric complex. Taken together, these results suggest that DDX1 acts as a cellular cofactor by promoting oligomerization of Rev on the RRE.

Introduction

Rev, a key regulatory protein of human immunodeficiency virus (HIV) type 1, activates nuclear export of unspliced and partially spliced viral mRNAs, which encode the RNA genome and the genes for the structural proteins Gag, Pol and Env, respectively (reviewed in Ref. 1). Rev binds to the Rev response element (RRE), a highly conserved region of the viral mRNA, which contains a single

*Corresponding author. E-mail address: millar@scripps.edu.

Abbreviations used: AMP-PNP, adenylyl-imidophosphate; ARM, arginine-rich motif; A555, Alexa Fluor 555; RRE, Rev response element; TIRF, total internal reflection fluorescence; HIV, human immunodeficiency virus; wt, wild type.

high-affinity binding site for Rev, although as many as eight Rev molecules can bind to a single RRE.[2–4] In fact, binding of a single Rev to the RRE is incapable of activating mRNA export, indicating that oligomerization of Rev on the RRE is essential for Rev function.[5,6] Further, while Rev is the central player, a number of cellular proteins also contribute to nucleocytoplasmic export of viral mRNAs and enhance Rev function.[7] Because Rev-mediated RNA export is essential for viral replication, the Rev–RRE complex is a potential therapeutic target for treatment of HIV/AIDS. However, owing to the complexity of the Rev pathway and the many macromolecular interactions in which it participates, effective therapies that target Rev have yet to be realized.

The human DEAD box protein DDX1 has been implicated as a cellular cofactor of Rev.[8,9] DEAD box proteins typically function as ATP-dependent RNA helicases and are involved in many aspects of RNA metabolism, including ribosome biogenesis, RNA splicing, translation and RNA degradation.[10,11] DDX1 is known to be required for efficient Rev function and proper nuclear localization of Rev in mammalian cells[8] and human astrocytes.[9] DDX1 has also been shown to interact with the N-terminus of Rev in yeast and mammalian two-hybrid systems.[8] Direct physical interactions between DDX1 and Rev and between DDX1 and the RRE were subsequently confirmed by *in vitro* binding studies.[12] In addition, silencing of DDX1 in HIV-1-infected HeLa cells drastically reduces virus particle production.[12] Taken together, these results establish that DDX1 is a key cellular cofactor of Rev, essential for Rev function and virus replication. However, the mechanism by which DDX1 acts to promote Rev function is not understood. More generally, the role that DEAD box proteins play in ribonucleoprotein assembly and nucleocytoplasmic transport of retroviral RNA is largely unexplored.

Since oligomeric assembly of Rev on the RRE is required for nuclear export of HIV mRNAs, we hypothesized that DDX1 may act as a cellular cofactor by assisting in the oligomerization process. Here, we test this hypothesis by using a single-molecule fluorescence spectroscopic method to observe individual steps in Rev–RRE assembly[13] in the presence of DDX1. Binding of up to eight Rev monomers on a single RRE was observed, and the presence of DDX1 significantly enhanced this assembly. The effect of DDX1 on Rev–RRE assembly was also examined in the presence of ADP or the non-hydrolyzable ATP analog adenylyl-imidophosphate (AMP-PNP). The rate constants for Rev monomer binding and dissociation were determined for each step of assembly, revealing the effect of DDX1 and nucleotide cofactors at specific points on the assembly pathway. These measurements were performed across a range of DDX1 concentrations to determine whether DDX1 promotes oligomeric assembly by interacting with Rev or the RRE, which have different affinities for DDX1. In addition, we tested the effect of DDX1 on an oligomerization-deficient Rev mutant. Our results demonstrate that DDX1 strongly promotes oligomerization of Rev on the RRE, explaining why DDX1 is required for efficient Rev function.

Results

Experimental system

Previously, we used total internal reflection fluorescence (TIRF) microscopy to monitor the assembly of fluorescently labeled Rev on single RRE molecules immobilized on a quartz surface. Individual Rev binding and dissociation steps were directly observed in real time as discrete jumps in fluorescence intensity from the surface-bound complexes. Statistical analysis of many fluorescence intensity trajectories recorded during individual assembly reactions provided detailed information on the stoichiometry and kinetics of the Rev–RRE interaction.[13] Here, we use the same method to investigate binding of Rev to the RRE in the presence of DDX1 and nucleotide cofactors (Fig. 1). One modification of the present study was to use the full 351-nt RRE instead of the truncated RRE construct used previously. The truncated RRE was only capable of binding up to four Rev monomers, whereas the full RRE binds up to eight monomers (see below), allowing us to examine higher-order binding events during Rev–RRE assembly. Full-length RRE was generated by *in vitro* transcription, biotinyated at the 5′ end and immobilized on a polyethylene-glycol-treated quartz surface coated with streptavidin. The fluorophore labeling site within the Rev protein was also different than that in the previous study. For this study, both native cysteines of Rev were mutated to serine, and a single cysteine residue used for labeling was introduced into an N-terminal extension, which also contained the His_6 tag used for affinity purification. We chose to label the Rev construct at this position to ensure that the labeling would not affect the native function of the protein. Apart from these changes, Rev was labeled with Alexa Fluor 555 (A555) and purified as described previously.[13] Similarly, the single-molecule TIRF data were acquired and processed as in the previous study.

To validate the new reagents, we first examined a binary system consisting of labeled Rev and full-length RRE (no DDX1 present). Typical fluorescence intensity trajectories (time traces) reveal discrete and abrupt transitions between states exhibiting different fluorescence intensities, reflecting spontaneous

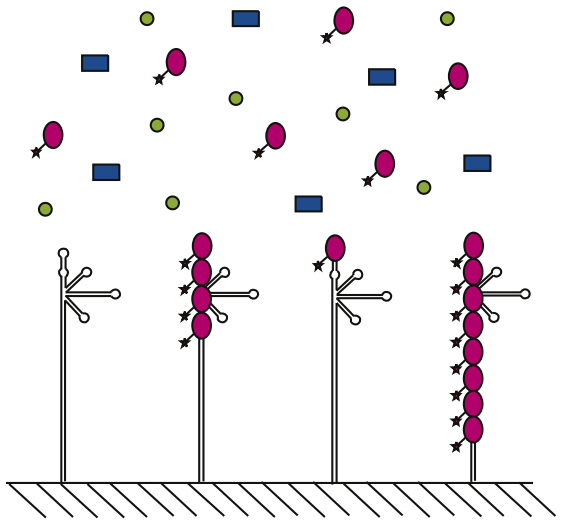

Fig. 1. Schematic of Rev–RRE assembly in the single-molecule experimental setup. The RRE is immobilized on a quartz slide, and fluorescently labeled Rev monomers (pink ovals) are free in solution. Up to eight Rev monomers can bind and dissociate from the immobilized RRE, with each step registered as a jump in fluorescence intensity. Assembly of Rev on the RRE can also be observed when DDX1 (blue rectangles) and nucleotide cofactors (ADP or AMP-PNP, green circles) are present in solution.

binding and dissociation events (Fig. 2a). The jump size distribution compiled from >20,000 individual trajectories shows that the most likely jump size is ~100 camera counts, corresponding to the average fluorescence intensity of a single Rev monomer under the experimental conditions (Fig. 3a). This is consistent with our previous conclusion obtained using a truncated RRE construct that Rev monomers bind to the RRE one at a time.[13] An intensity histogram compiled from the entire set of trajectories reveals discrete peaks corresponding to the 1:1, 2:1 and 3:1 Rev–RRE complexes and a tail extending to higher intensities (Fig. 4a). The histogram reflects the relative frequency of occurrence of the different intensity states sampled during *both* binding and dissociation events. To estimate the statistical frequencies of binding and dissociation events separately, including those hidden in the tail of the histogram, we assigned specific intensity ranges to each stoichiometry state and classified individual transitions accordingly. The resulting event frequencies, compiled from a total of 53,350 transitions, are shown in Fig. 5a. Generally, the statistical frequencies of a given binding transition and the corresponding dissociation transition are equivalent, as expected for a reversible system at equilibrium. Binding of up to eight Rev monomers to the full-length RRE is observed, consistent with previous reports,[2–4] although the higher-order Rev monomer binding events are observed less frequently than the early binding events. This is expected for a sequential monomer binding pathway because the higher-order complexes necessarily form more slowly than lower-order complexes and, as a consequence, are underrepresented during the finite recording time of the TIRF measurements (20 s). Hence, the event frequencies and the intensity histogram do not reflect the true equilibrium distribution of species. Nevertheless, these observable parameters still report changes in the Rev–RRE assembly pathway under various conditions, as shown later.

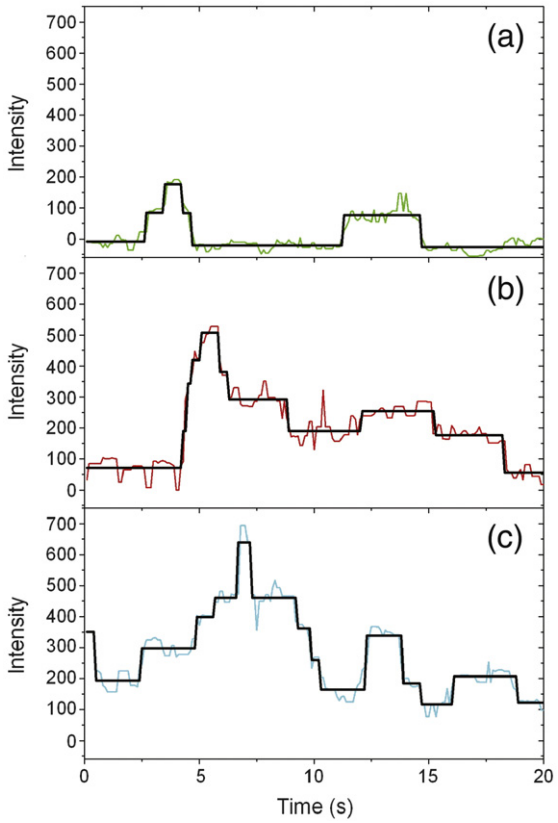

Fig. 2. Fluorescence intensity trajectories recorded during Rev–RRE assembly. One Rev monomer bound to the RRE emits a fluorescence intensity of ~100 camera counts on average. (a) The green trace is a typical intensity time trace for Rev–RRE-binding activity without DDX1 present. Up to two Rev monomers are bound to the RRE in this particular trace. Other traces reveal more bound Rev monomers, but these are observed less frequently. (b) The red trace is a typical intensity time trace in the presence of 150 nM DDX1. Up to five Rev monomers are bound to the RRE in this trace. (c) The blue trace is a typical intensity time trace in the presence of 150 nM DDX1 and 1 mM AMP-PNP. Up to seven Rev monomers are bound to the RRE in this trace. The black lines show fits to the intensity trajectories using a custom software. The baseline level in (b) and (c) is the same as in (a).

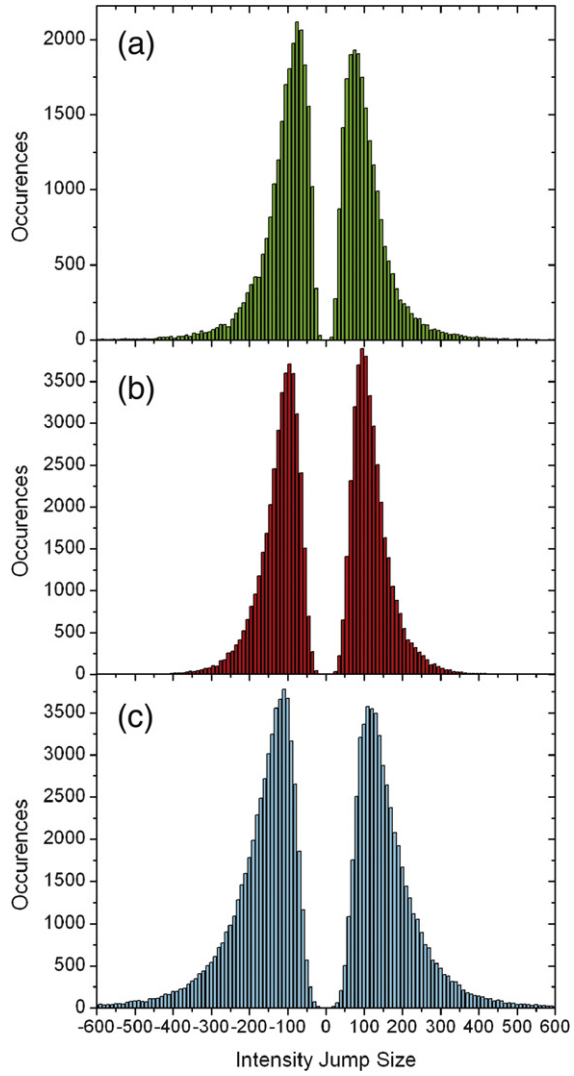

Fig. 3. Distribution of intensity jump sizes observed during Rev–RRE assembly. (a) Jump size distribution of the binary Rev–RRE system compiled from 45,071 events. The mean jump size is 110 camera counts for upward transitions and −110 camera counts for downward transitions. (b) Jump size distribution in the presence of 150 nM DDX1 compiled from 78,128 events. The mean jump size is 121 camera counts for upward transitions and −124 camera counts for downward transitions. (c) Jump size distribution in the presence of 150 nM DDX1 and 1 mM AMP-PNP compiled from 109,760 events. The mean jump size is 110 camera counts for upward transitions and −110 camera counts for downward transitions.

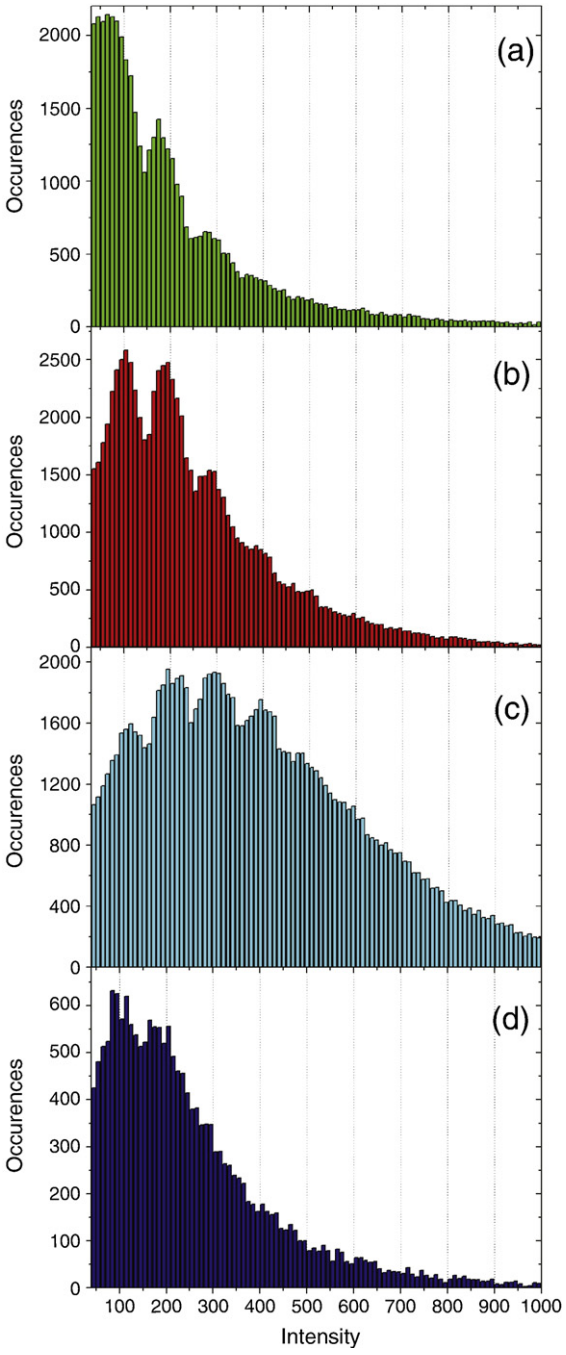

Fig. 4. Fluorescence intensity histograms compiled from intensity trajectories recorded during individual Rev–RRE assembly reactions. (a) Histogram for wt Rev and RRE compiled from 53,350 individual transitions. (b) Histogram for wt Rev and RRE in the presence 150 nM DDX1 compiled from 82,283 transitions. (c) Histogram for wt Rev and RRE in the presence of 150 nM DDX1 and 1 mM AMP-PNP compiled from 109,760 transitions. (d) Histogram for wt Rev and RRE in the presence of 150 nM DDX1 and 1 mM ADP compiled from 19,700 transitions.

The presence of photobleached Rev molecules would result in an underestimate of the stoichiometry of the Rev–RRE complex because such molecules would not be detected in our TIRF measurements. However, the rate of photobleaching of the A555 dye is slow ($0.0085 \pm 0.0001\ s^{-1}$) under our experimental conditions.[13] Moreover, photobleaching can only occur in the shallow evanescent

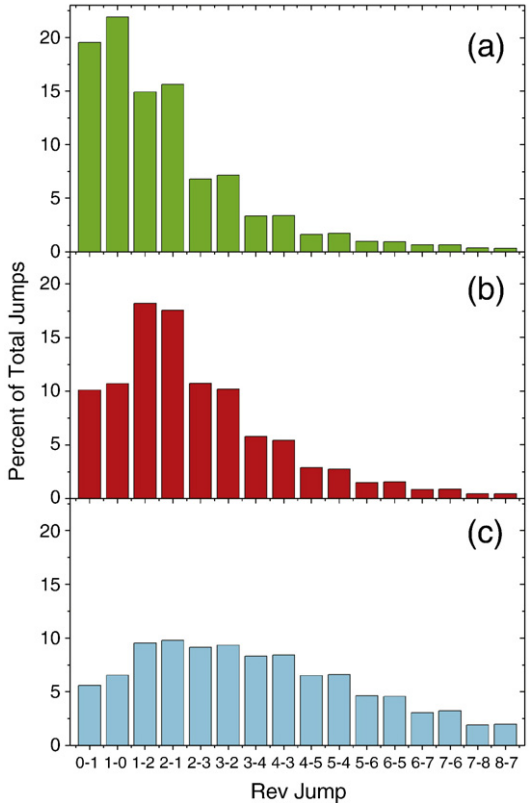

Fig. 5. Event frequencies. Numbers on the horizontal axis correspond to the number of Rev monomers bound before and after the event (e.g., 1–2 corresponds to a second Rev binding after one had been bound to the RRE). The heights of the bars correspond to the frequency of occurrence of each event expressed as a fraction of the total number of transitions. (a) Rev and RRE. (b) Rev and RRE in the presence of 150 nM DDX1. (c) Rev and RRE in the presence of 150 nM DDX1and 1 mM AMP-PNP.

field (~100 nm deep), whereas labeled Rev molecules are free to diffuse in and out of the evanescent field. Based on a reasonable estimate of the translational diffusion coefficient of Rev (1.2×10^{-6} cm^2 s^{-1}), the time required to traverse the 100-nm evanescent field before binding to the immobilized RNA, assuming a diffusive random walk, is expected to be on the order of tens of microseconds. Given the slow rate of photobleaching and the short transit time, the fraction of Rev molecules that will photobleach before binding to the RRE is predicted to be inconsequentially small. Some Rev molecules do photobleach *after* binding to the RRE because they remain in the evanescent field for a longer period of time. This is responsible for the slight excess of downward intensity transitions evident in Fig. 3a. These photobleaching events are taken into account in the analysis of Rev dissociation kinetics.

Kinetic information on each of the Rev binding and dissociation steps was obtained by compiling the distribution of dwell times for each stoichiometry state prior to an upward or downward intensity transition, as described previously.[13] Examples of the resulting dwell-time histograms are shown in Fig. 6a and c. Apart from the initial binding step, each of the histograms can be fitted well with a single-exponential decay (R^2 values between 0.95 and 0.99). The dwell-time histogram for the first Rev binding event requires two exponentials for a good fit ($R^2=0.99$), revealing fast (first-order rate constant of 0.55 ± 0.12 s^{-1}) and slow (first-order rate constant of 0.12 ± 0.01 s^{-1}) kinetic phases with roughly equal amplitudes (56% and 44%, respectively) (Fig. 6a). A second kinetic phase, present only during the initial Rev binding step, was also observed in our previous study utilizing a truncated RRE construct.[13] The biphasic kinetics could reflect two conformations of the RRE or two populations of Rev monomers, as discussed in more detail later. The binding and dissociation rate constants for each stoichiometry state obtained from the exponential fits are presented in Figs. 7a and 8a, respectively (only the slower rate is shown for the first binding step, as explained later in Discussion). Note that the slow rate of dye photobleaching is taken into account in calculation of the dissociations rate constants.[13] The binding data are presented as bimolecular association rate constants. Clearly, Rev monomers bind more rapidly to the RRE as assembly proceeds. A maximum association rate constant of $\sim1\times10^9$ M^{-1} s^{-1} is in the range expected for diffusion-controlled binding of a small protein such as Rev. In addition, it is evident that the higher-order Rev–RRE complexes also dissociate more rapidly than the lower-order complexes (Fig. 8a). The binding and dissociation rate constants for the first four Rev monomers are similar to those determined previously using the truncated RRE construct.[13] Overall, the full-length RRE recapitulates the behavior of the truncated construct used previously while also providing detailed kinetic information on the later stages of Rev–RRE complex assembly.

DDX1 promotes oligomerization of Rev on the RRE

The same approach was used to monitor Rev–RRE assembly reactions in the presence of DDX1 (150 nM), which was unlabeled. The intensity trajectories again reveal discrete jumps as Rev monomers bind to or dissociate from the immobilized RRE (Fig. 2b). However, it is readily apparent from comparison of Fig. 2a and b that higher intensity states are sampled in the presence of DDX1. This difference is also manifested in the intensity histogram compiled from >20,000 individual trajectories recorded in the presence of 150 nM DDX1. The histogram reveals a significant shift toward higher intensity states (Fig. 4b) compared

with the binary Rev–RRE system (Fig. 4a). The higher intensity is not due to a direct effect of DDX1 on the A555 dye, since there is little change in fluorescence intensity as A555-labeled Rev is titrated with DDX1 in solution, even though fluorescence anisotropy measurements indicate that DDX1 binds to Rev.[12] Consistent with this, DDX1 has little effect on the average jump size observed in the single-molecule intensity trajectories (Fig. 3b). In addition, TIRF measurements performed in the absence of the immobilized RRE indicate that the presence of DDX1 does not cause a measurable increase in the nonspecific adsorption of Rev to the quartz surface (results not shown). Hence, the higher intensity states populated in the presence of DDX1 must reflect a larger number of Rev monomers binding to the RRE. Further, statistical analysis of the transition frequencies reveals significantly more higher-order Rev–RRE binding events in the presence of DDX1 (Fig. 5b). While more Rev monomers are bound to the RRE in the presence of DDX1, they still bind one at a time (Fig. 3b).

Kinetic information on the various Rev binding and dissociation steps was obtained using dwell-time analysis, as before. Interestingly, the dwell-time histogram for the first Rev monomer binding step is well fit by a single-exponential decay (Fig. 6b), in contrast to the two rates with roughly equal amplitudes observed in the absence of DDX1 (described above). Notably, the relative number of initial Rev monomer binding events (compared to the total number of binding events) is also reduced by ~50% in the presence of DDX1 (Fig. 5b). Therefore, we suspect that the second kinetic phase, present without DDX1, is due to a nonproductive binding mode, in which subsequent Rev monomers are unable to bind to the RRE. This nonproductive nucleation results in reduced oligomerization and an excess of single monomer assembly states in the absence of DDX1 (Fig. 5a, leftmost column). Apparently, DDX1 is able to suppress these nonproductive nucleation events, promoting higher-order assembly of Rev on the RRE. DDX1 also accelerates binding of the first Rev monomer but has little effect on the rates at which subsequent Rev monomers bind to the RRE (Fig. 7b). Likewise, DDX1 has relatively little effect on the dissociation rate constants of any of the Rev–RRE complexes (Fig. 8b), indicating that DDX1 does not stabilize any of the complexes.

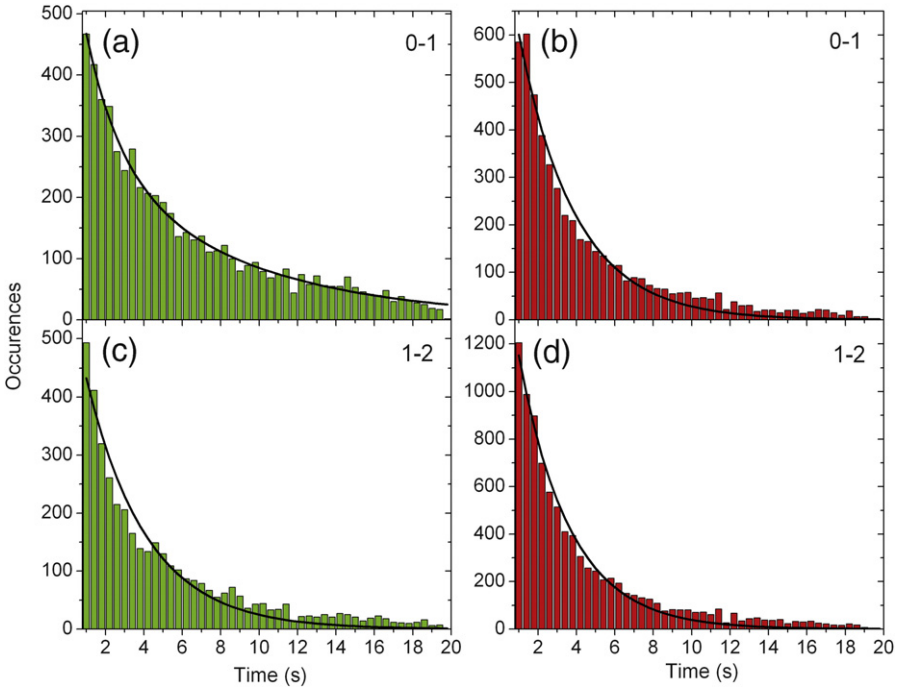

Fig. 6. Dwell-time histograms for the first two steps of Rev–RRE assembly without DDX1 present (a and c) or with 150 nM DDX1 present (b and d). The numbers in the top right-hand corners of each plot indicate the number of Rev monomers bound before and after the event. For the first Rev binding event without DDX1 present (a), the continuous line is a fit to a double-exponential decay, with $k_1 = 0.55 \pm 0.12\ s^{-1}$, $k_2 = 0.12 \pm 0.01\ s^{-1}$ and $R^2 = 0.99$. The relative amplitudes of these kinetic phases are 56% and 44%, respectively. The continuous lines in the other panels are all single-exponential fits, with $k = 0.34 \pm 0.01\ s^{-1}$ and $R^2 = 0.98$ (b), $k = 0.32 \pm 0.01\ s^{-1}$ and $R^2 = 0.96$ (c) and $k = 0.38 \pm 0.01\ s^{-1}$ and $R^2 = 0.99$ (d). All rate constants given here are first-order rate constants determined from the exponential fits.

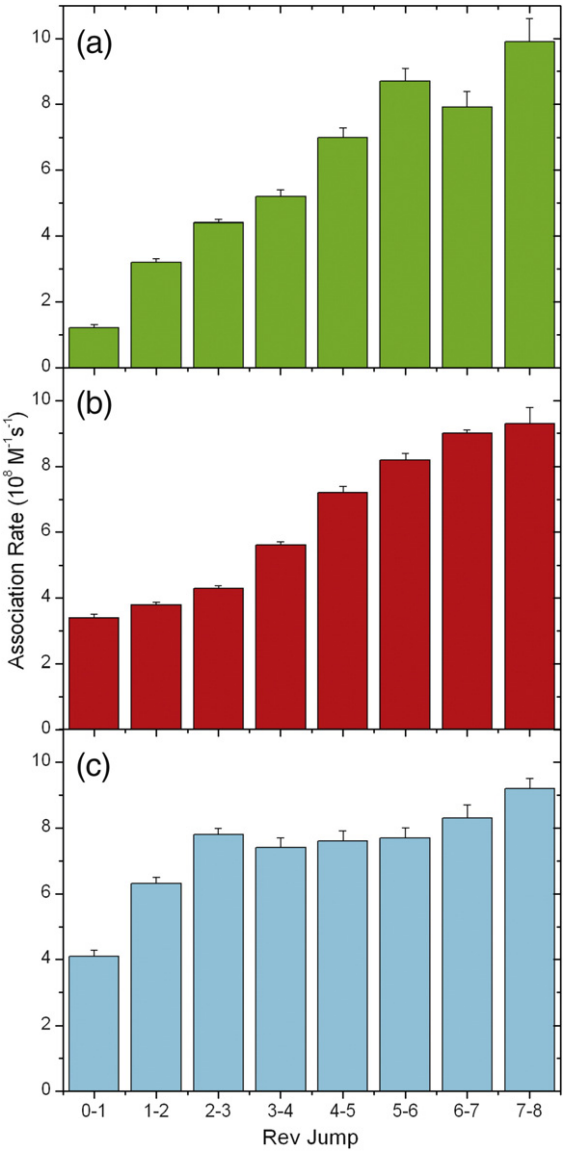

Fig. 7. Association rate constants for Rev–RRE binding events. Numbers on the horizontal axis correspond to the number of Rev monomers bound before and after the binding transition. The heights of the bars correspond to the bimolecular association rate constant for the given binding step. (a) Rev and RRE. (b) Rev and RRE in the presence of 150 nM DDX1. (c) Rev and RRE in the presence of 150 nM DDX1 and 1 mM AMP-PNP.

Effect of nucleotides on Rev–RRE assembly in the presence of DDX1

DEAD box proteins typically function as ATP-dependent RNA helicases.[10] Beyond helicase activity, nucleotide binding can induce a conformational change that may affect other properties of the protein as well. To investigate whether such nucleotide-induced conformational changes play any role in the ability of DDX1 to promote oligomerization of Rev on the RRE, we repeated the single-molecule TIRF measurements in the presence of DDX1 and either ADP or the non-hydrolyzable ATP analog AMP-PNP. Since DEAD box proteins actively hydrolyze ATP, we used AMP-PNP to avoid any complications associated with nucleotide hydrolysis. The intensity histogram obtained in the presence of 150 nM DDX1 and 1 mM ADP (Fig. 4d) is similar to that obtained in the presence of DDX1 alone (Fig. 4b), indicating that ADP does not promote any further increase in Rev oligomerization on the RRE. In contrast, the intensity histogram recovered in the presence of 150 nM DDX1 and 1 mM AMP-PNP (Fig. 4c) reveals a pronounced shift toward higher-order Rev–RRE complexes compared to the results obtained when DDX1 is absent (Fig. 4a) or when only DDX1 is present (Fig. 4b). Moreover, higher-order Rev–RRE binding events are observed more frequently when both DDX1 and AMP-PNP are present (Fig. 5c), with Rev monomers still binding to the RRE one at a time (Fig. 3c). Further, while DDX1 and AMP-PNP have little effect on the dissociation rates of any of the complexes (Fig. 8c), the association rates for the second, third and fourth Rev monomer binding events are markedly accelerated compared to DDX1 alone (Fig. 7c). While the rates of subsequent Rev monomer binding steps are not significantly affected by DDX1 and AMP-PNP, the acceleration during the early assembly steps leads to a higher probability for the higher-order events to occur (Fig. 5c). Importantly, experiments carried out in the presence of AMP-PNP but without DDX1 do not exhibit these effects; rather, the results are similar to those found for the binary Rev–RRE system. Taken together, these results demonstrate that DDX1 is most efficient in promoting oligomerization of Rev on the RRE when bound by AMP-PNP.

DDX1 targets Rev rather than the RRE to promote oligomeric assembly

In principle, the ability of DDX1 to promote oligomerization of Rev on the RRE could be due to an interaction between DDX1 and Rev or between DDX1 and the RRE because DDX1 is known to bind to both of these targets.[12] To distinguish these possibilities, we determined the Rev oligomer size $\overline{O}$ (average number of Rev monomers bound to the RRE) for varying concentrations of DDX1 using the formula:

$$\overline{O} = \frac{\sum_{n=1}^{8} nE_n}{\sum_{n=1}^{8} E_n}$$

where n is the number of Rev monomers bound to the RRE and E_n is the number of events for that oligomer

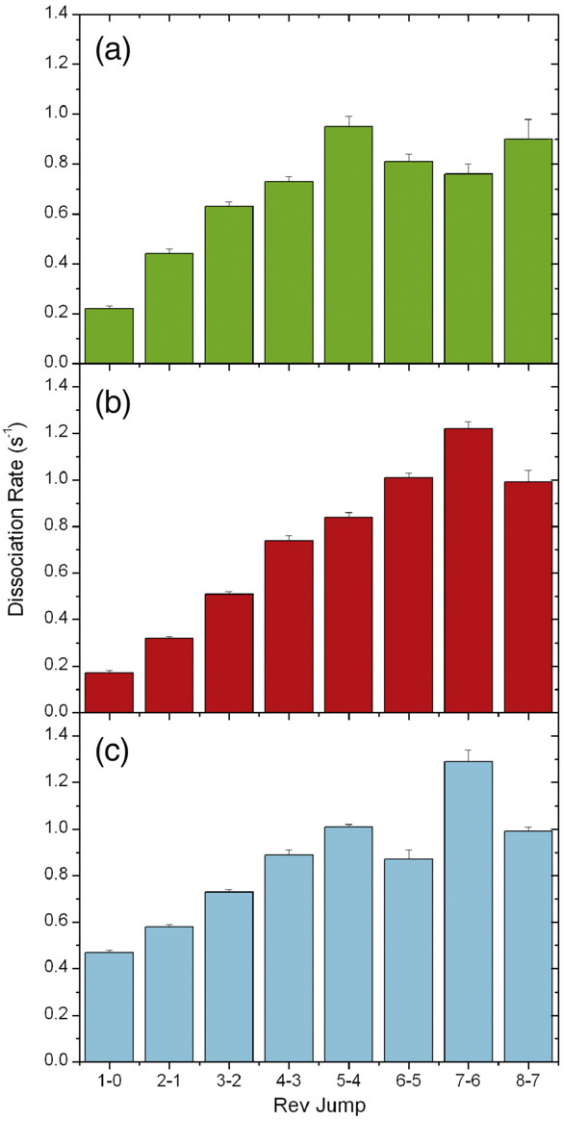

Fig. 8. Dissociation rate constants for individual Rev–RRE stoichiometries. The numbering scheme on the horizontal axis is the same as in Fig. 7. The heights of the bars correspond to the dissociation rate constants obtained from dwell-time analysis after correction for the slow rate of A555 photobleaching. (a) Rev and RRE. (b) Rev and RRE in the presence of 150 nM DDX1. (c) Rev and RRE in the presence of 150 nM DDX1 and 1 mM AMP-PNP.

size. It should be noted that $\overline{O}$ represents the apparent number of Rev monomers bound to the RRE because the event frequencies E_n do not reflect true equilibrium populations, as noted above. As shown in Table 1, $\overline{O}$ is strongly dependent on DDX1 concentration (in the presence of 1 mM AMP-PNP), almost doubling as the DDX1 concentration is increased from 0 to 150 nM. Clearly, the full effect of DDX1 on promoting oligomerization of Rev on the RRE occurs between

Table 1. Effect of DDX1 concentration on oligomerization of Rev on the RRE

DDX1 concentration (nM)	Average Rev oligomer size[a]
0	2.19
10	2.24
50	3.81
150	3.73

[a] The average Rev oligomer size is defined in the text.

DDX1 concentrations of 10 and 50 nM. Interestingly, bulk *in vitro* fluorescence experiments have shown that DDX1 binds Rev with a K_d value of 36 nM, whereas it binds RNA much more weakly, with a K_d value of 310 nM.[12] On the basis of these K_d values, we anticipate that 58% of Rev molecules will be bound by DDX1 at a DDX1 concentration of 50 nM, whereas only 13% of RRE molecules will be bound by DDX1. Hence, it is likely that DDX1 targets and interacts with Rev rather than the RRE in order to promote oligomeric Rev–RRE assembly.

DDX1 restores oligomerization activity of a Rev mutant

To further investigate the role that DDX1 and AMP-PNP play in facilitating Rev–RRE assembly, we repeated the TIRF measurements with an oligomerization-deficient Rev mutant (V16D/I55N). As shown in Fig. 9a, V16D/I55N Rev is unable to form higher-order complexes on the full-length RRE, consistent with previous results obtained with a truncated RRE construct.[13] The only peak present in the intensity histogram corresponds to a single Rev monomer bound to the RRE. Moreover, the dwell-time histogram for Rev monomer binding exhibits single-exponential kinetics with a bimolecular association rate of $(3.0\pm0.1)\times10^8$ M^{-1} s^{-1} (results not shown), similar to the fast phase seen with wild-type (wt) Rev. Notably, when 150 nM DDX1 is added, the Rev mutant is able to form higher-order complexes with the RRE (Fig. 9b), although the effect of DDX1 is not as pronounced as that with wt Rev (Fig. 4b). Similarly, upon subsequent addition of 1 mM AMP-PNP, oligomerization of V16D/I55N Rev is enhanced even further (Fig. 9c), producing an intensity histogram that is similar to that observed with wt Rev under the same conditions (Fig. 4c). Thus, DDX1 in the presence of AMP-PNP is able to substantially overcome a deficiency in Rev oligomerization in order to drive Rev–RRE assembly.

Discussion

In this study, we have shown that the human DEAD box DDX1 promotes oligomerization of Rev

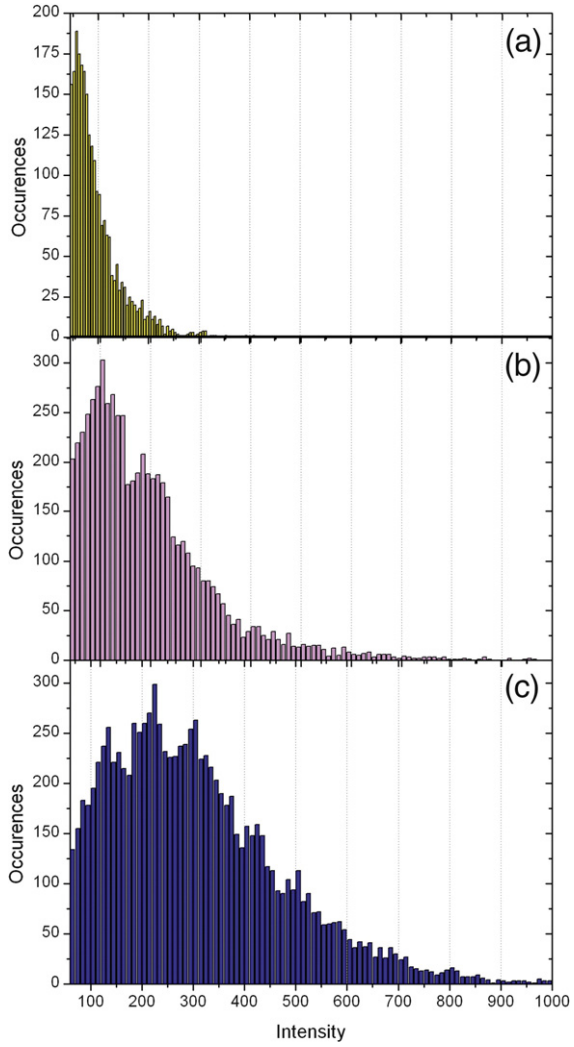

Fig. 9. Fluorescence intensity histograms compiled from intensity trajectories recorded during individual Rev–RRE assembly reactions. (a) Histogram for V16D/I55N Rev and RRE compiled from 5100 transitions. (b) Histogram for V16D/I55N Rev and RRE, with 150 nM DDX1 present, compiled from 9870 transitions. (c) Histogram for V16D/I55N Rev and RRE, with 150 nM DDX1 and 1 mM AMP-PNP present, compiled from 17,300 transitions.

on the RRE, a process that is essential for the nuclear export of unspliced and singly spliced HIV mRNA transcripts. Using the single-molecule fluorescence assay, we have shown that up to eight Rev monomers assemble on the full-length RRE, each binding one at a time. While this assembly can proceed in the absence of DDX1, early binding events are accelerated when DDX1 is present, and subsequent binding events are observed to occur more frequently as a result. Moreover, the impact of DDX1 on Rev–RRE assembly is sensitive to the presence of nucleotide cofactors, with the non-hydrolyzable ATP analog AMP-PNP producing larger effects than ADP. Under optimal conditions (1 mM AMP-PNP), DDX1 is able to restore the oligomerization activity of a Rev mutant that is otherwise incapable of assembling on the RRE beyond a monomeric complex.

One of the most significant findings of our study was the observation that the first Rev monomer binds to the RRE with two distinct kinetic phases, whereas all subsequent Rev monomer binding steps display single-exponential kinetics (Fig. 6a and c). Notably, in the presence of DDX1, one of the kinetic phases during nucleation is suppressed (Fig. 6b). There are two models that can explain these observations. In one model, the RRE can adopt two distinct conformations, both of which can bind a single Rev monomer, but only one conformation allows for subsequent oligomerization of Rev on the RRE. Since DEAD box proteins usually possess duplex unwinding and RNA annealing activities,[10,11] it is possible that DDX1 refolds the RRE and thereby suppresses the nonproductive channel. Although the helicase activity of DDX1 has yet to be established, DDX1 is known to bind to the RRE, albeit rather weakly (K_d = 310 nM[12]). In the other model, Rev monomers can adopt two distinct conformations in solution, only one of which is competent to oligomerize on the RRE. It is assumed that the two populations exist in a reversible equilibrium. According to this model, DDX1 binds to and stabilizes the productive population of Rev monomers, while mutations within Rev favor the nonproductive population. The first model is consistent with certain aspects of our data. For example, some DEAD box helicases promote RNA strand annealing in the absence of nucleotides,[14,15] while others require ATP binding.[16] Other DEAD box helicases unwind RNA duplexes in the presence of ATP, but do not require ATP hydrolysis.[17–19] Hence, it is conceivable that DDX1 could refold the nonproductive RRE conformation in the absence of nucleotides and that this activity would be further enhanced in the presence of AMP-PNP, but not ADP. These possibilities are consistent with our data and favor the first model. The second model is supported by the observation that DDX1 binds tightly to Rev in solution, with a K_d value of 36 nM.[12] In fact, we find that 50 nM DDX1 is sufficient to fully stimulate oligomerization of Rev on the RRE, which is consistent with the reported K_d value for the DDX1–Rev interaction. However, relatively few RRE molecules are expected to be bound and refolded by DDX1 under these conditions based on the reported K_d for the DDX1–RRE interaction.[12] Moreover, the second model provides a rationale for the observation that the V16D/I55N Rev mutant binds the

RRE as a monomer and displays just a single fast kinetic phase. The slow binding phase observed with wt Rev is attributed to the productive population of Rev monomers. The second model also explains why DDX1 restores oligomerization activity of the V16D/I55N Rev mutant, since DDX1 is postulated to stabilize the productive population of Rev monomers. In contrast, it is difficult to explain how DDX1 is able to compensate for protein mutations if it is acting solely on the RNA (first model). Overall, we favor the model of two Rev monomer populations because it can readily explain all of our observations. Nevertheless, we cannot formally rule out the possibility that DDX1 acts by refolding the RRE structure, although this appears unlikely.

The model of two Rev monomer populations is consistent with all of our results, but what is the origin of the population that binds nonproductively to the RRE and why is this species suppressed when DDX1 is present? The recently reported crystal structure of a Rev dimer offers some clues.[20] Only the N-terminal domains of each Rev monomer are visible in this structure, indicating that the C-terminal domains are disordered in the crystal. Nevertheless, the structure is informative because the N-terminal domain contains the RNA-binding and oligomerization functions of Rev. Within each monomer, two α-helices (α_1 and α_2) lie side by side, connected by an unstructured loop, forming a planar hairpin-like structure with two distinct faces, denoted A and B (Fig. 10). Monomer–monomer contacts in the dimer occur between the pronged ends of the helical hairpins, utilizing the A interfaces of each monomer. Notably, within each monomer, the hydrophobic patches mediating dimerization are

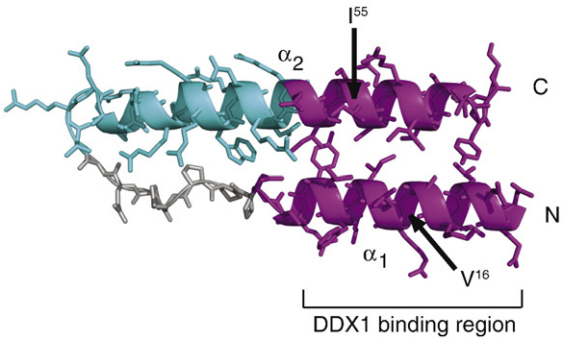

Fig. 10. Helical hairpin structure of the N-terminal domain of Rev, as observed in the crystal structure of a Rev dimer.[20] The ARM responsible for RNA binding is colored cyan, and the oligomerization regions are colored pink. The location of the DDX1 binding region (amino acids 10 through 24), as defined by mammalian two-hybrid studies, is indicated.[8] The precise location of the DDX1 binding site within this region is unknown. The positions of residues V16 and I55 are also indicated. This figure was adapted from Ref. 20.

physically distinct from the arginine-rich motif (ARM) responsible for RNA binding (Fig. 10). Given the segregation of these regions, it is conceivable that a Rev monomer could be properly folded in the ARM, allowing for RNA binding, while being partially unfolded at the pronged end of the hairpin, inhibiting oligomerization. Thus, we speculate that the nonproductive population of Rev monomers identified in our study arises from such a partially folded species. One or both of the α-helices may be partially unwound, or they may not pack optimally, in either case disrupting the A and/or B surface required for oligomerization. Consistent with this suggestion, we note that the V16 and I55 residues are located in the α_1 and α_2 helices, respectively (Fig. 10) and that replacement of both residues with polar amino acids (V16D/I55N mutations) shifts all Rev monomers into the nonproductive form. CD spectroscopic data also indicate that the V16D/I55N double mutation disrupts the secondary structure of Rev.[21] Partial unfolding within the N-terminal domain of Rev is not surprising, given that the C-terminal domain is totally disordered in the Rev dimer crystal structure.[20]

The productive population of Rev monomers, capable of RNA binding and oligomerization, likely corresponds to the helical hairpin structure observed in the Rev dimer crystal. Interestingly, the results of yeast two-hybrid screening indicate that DDX1 interacts with the N-terminus of Rev,[8] somewhere between residues 10 and 24. This region corresponds to the pronged end of the helical hairpin (Fig. 10), suggesting that DDX1 might recognize and stabilize the helical hairpin conformation of Rev. If so, DDX1 would function as a protein chaperone, delivering Rev monomers to the RRE in a conformation that facilitates Rev–Rev interactions on the RRE. AMP-PNP may enhance the chaperone activity by inducing a distinct conformation of DDX1 that interacts more favorably with the Rev hairpin. DEAD box proteins contain two RecA-like domains joined by a flexible hinge.[22] The intervening cleft is open in the absence of nucleotides, whereas ATP promotes closing of the two domains.[22] Presumably, AMP-PNP will induce a closed conformation of DDX1, which appears to be more effective in stabilizing the Rev hairpin. The role of DDX1 in acting as a protein chaperone is a previously unrecognized function of DEAD box proteins.

While our results suggest that DDX1 presents Rev to the RRE in a conformation that facilitates oligomerization, it is unclear whether DDX1 remains stably bound once the Rev–Rev contacts have formed, since DDX1 is not directly visualized in our experiments. Since the DDX1 binding region of Rev overlaps with the oligomerization region (Fig. 10), it is possible that DDX1 dissociates from Rev as stable Rev–Rev interactions are established,

especially as the affinity of the Rev–DDX1 interaction (K_d = 36 nM[12]) is less than that of the Rev–Rev interaction (K_d ~1.5 nM for the second monomer binding step based on the association and dissociation rates measured here). Moreover, the dissociation rates of the various Rev–RRE assembly intermediates are unchanged in the presence of DDX1 (Fig. 8), which also suggests that DDX1 is not stably bound during Rev–RRE assembly. Alternatively, since the precise location of the DDX1 binding site on Rev and the mode of binding are both unknown, it is formally possible that DDX1 remains stably bound as part of a Rev–DDX1–RRE ternary complex. Future two-color TIRF experiments in which DDX1 is also fluorescently labeled should reveal whether DDX1 dissociates after delivering Rev to the RRE or remains bound as well.

Previous studies have shown that DDX1 is required for efficient Rev function. For example, depletion of DDX1 in mammalian cells results in a decreased amount of unspliced viral mRNA in the cytoplasm and a correspondingly increased amount of spliced *versus* unspliced RNA in the nucleus, both effects indicating a reduction in Rev function.[8] Since oligomerization of Rev on the RRE is essential for the nuclear transport of unspliced and partially spliced viral mRNAs from the nucleus to the cytoplasm, the ability of DDX1 to promote this assembly process would result in more efficient nuclear export. Hence, our results suggest that DDX1 functions as a cellular Rev cofactor by promoting oligomeric assembly of Rev on the RRE.

Conclusions

We have carried out detailed single-molecule fluorescence experiments to dissect the role of DDX1 in Rev–RRE complex assembly. Our results clearly demonstrate that DDX1 promotes oligomerization of Rev on the RRE and that this effect is significantly increased in the presence of the ATP analog AMP-PNP. We propose that the Rev monomer structure is intrinsically dynamic in solution, with some monomers being capable of efficient oligomerization on the RRE, while others are unable to assemble beyond a 1:1 protein–RNA complex. Moreover, we suggest that DDX1 promotes oligomeric Rev–RRE assembly by stabilizing the correct Rev monomer structure. The precise structural difference between the two Rev monomer populations remains to be elucidated, and other types of single-molecule fluorescence experiments (such as fluorescence resonance energy transfer) should be useful in this regard. Overall, our results raise the intriguing possibility that cellular cofactors could promote Rev function by acting as protein chaperones.

Materials and Methods

RRE constructs

The full-length RRE construct (351 nt) was generated by *in vitro* transcription and subsequently biotinylated at the 3′ end for surface attachment. Details of the transcription and biotinylation protocols are described elsewhere.[23]

Rev labeling and purification

Purified recombinant Rev proteins were based on the sequence: MGHHHH $^{-10}$HHS**C**GLFKRH ^{1}MAGRSGD**S**DE ^{11}DLLKA**V**RLIK ^{21}FLYQSN**P**PPN ^{31}PEGTRQARRN ^{41}RRRRWRERQR ^{51}QIHS**I**SERIL ^{61}STYLGRSAEP ^{71}VPLQLPPLER ^{81}LTLD**S**NED**S**G ^{91}TSGTQGVGSP ^{101}QILVESPTVL ^{111}ESGTKE. This construct is mutated from the native sequence at positions 85 and 89 (shown in bold), removing both native cysteine residues. Since both positions are well removed from the RNA binding region of Rev (amino acids 34–50), these mutations are not expected to impair the RNA-binding activity of the protein. In the numbering system, the sequence of wt Rev begins at residue 1. The N-terminal extension (residues −1 to −16) contains a 6-histidine tag used for affinity purification and a single cysteine residue at position −7 for fluorophore labeling (shown in bold type and underlined). An oligomerization-deficient Rev mutant contained additional V16D and I55N mutations[21] (amino acid positions are also shown in bold type). This construct is referred to as V16D/I55N Rev. All Rev constructs were expressed and purified as previously described.[21] Both purified recombinant proteins were then labeled with A555 at the single cysteine and further purified, as previously described.[13] Briefly, the labeled and unlabeled Rev proteins were separated by HPLC purification under denaturing conditions, and labeled proteins were subsequently refolded by equilibrium dialysis, aliquoted and stored at −80 °C prior to measurement. Mass spectral data confirmed that Rev was 100% labeled (Supplementary Information).

DDX1 protein expression and purification

A plasmid containing DDX1 was initially provided by the Godbout Lab (University of Alberta). The DDX1 gene was amplified using PCR and inserted into a modified pET22b expression vector (Novagen) for expression of full-length DDX1 protein with an N-terminal 6-histidine tag. BL21(DE3) gold *Escherichia coli* cells transformed with pET22-HT-DDX1 plasmid were grown in LB broth to an OD_{600} = 0.8 at 37 °C. Cell cultures were transferred to 30 °C, and DDX1 expression was induced by addition of 1 mM IPTG for 3 h . Cells were harvested by centrifugation and stored at −80 °C until ready for use. Harvested *E. coli* cells were resuspended in nickel column buffer [20 mM Tris (pH 7.9), 1 M NaCl, 10% glycerol, 0.1% Triton X-100, 12 mM imidazole and 10 mM β-mercaptoethanol], and the cell membranes were disrupted by sonication. Cell debris was removed by centrifugation, and the resulting lysate was treated with 5% polyethyleneimine (Sigma) to remove contaminating nucleic acids prior to affinity column purification using Ni-NTA resin (QIAGEN). Pooled

fractions containing DDX1 protein were dialyzed against Q column buffer [25 mM Tris (pH 8.8), 25 mM NaCl, 2 mM DTT and 1 mM ethylenediaminetetraacetic acid] and run over a 5-mL Hi-Trap Q HP Sepharose column (GE Healthcare). Pure DDX1 was dialyzed against 4 L of storage buffer [25 mM Hepes (pH 7.5), 175 mM KCl and 2 mM tris(2-carboxyethyl)phosphine] and stored at 4 °C.

TIRF microscopy

Measurements were performed using a custom-built, prism-based TIRF microscope. Complete details of the microscopy methods are described elsewhere.[13] Briefly, RRE molecules were immobilized on a quartz surface by biotin–streptavidin attachment. The surface was also modified with polyethylene glycol to minimize non-specific protein adsorption. Samples consisted of 100 pM biotinylated RRE, 1 nM Rev labeled with A555, DDX1 (0, 10, 50 or 150 nM) and AMP-PNP (0 or 1 mM) or ADP (0 or 1 mM) in 10 mM Hepes buffer (pH 7.5) containing 150 mM KCl, 10 mM K_2SO_4, 2 mM $MgCl_2$ and 2 mM DTT. Additionally, 1 mM propyl gallate was added to all samples as an oxygen scavenger. An argon-ion laser was used to excite the A555 fluorophores, and the resulting fluorescence was collected through a water immersion objective and detected on an electron-multiplying CCD camera (Andor).

TIRF data analysis

Fluorescence intensity trajectories (time traces) of individual Rev–RRE complexes were extracted from raw CCD camera movie files using a custom-written script described previously.[13] Custom programs (written in Matlab) were used to analyze the trajectories in order to identify discrete states with distinguishable fluorescence intensities and to identify the transition points between distinct intensity states, yielding the mean intensity and dwell time for each state sampled in the trajectory. These values were used to construct intensity and dwell-time histograms using data analysis and graphing software (Origin Lab). The dwell-time histograms for upward and downward transitions were fit to a single- or double-exponential function in order to calculate the corresponding rate constants for binding or dissociation of Rev.[13] The first-order binding rate constants obtained from the exponential fits were converted into second-order association rate constants by dividing them by the total Rev concentration (1 nM). For the downward transitions, the slow photobleaching rate of A555 was taken into account, as described previously.[13]

Supplementary materials related to this article can be found online at doi:10.1016/j.jmb.2011.04.026

Acknowledgements

We thank Edwin van der Schans and Edit Sperling for expert technical assistance. This research was supported by the US National Institutes of Health through P50 grant GM082545.

References

1. Pollard, V. W. & Malim, M. H. (1998). The HIV-1 Rev protein. *Annu. Rev. Microbiol.* **52**, 491–532.
2. Mann, D. A., Mikaelian, I., Zemmel, R. W., Green, S. M., Lowe, A. D., Kimura, T. *et al.* (1994). A molecular rheostat. Co-operative rev binding to stem I of the rev-response element modulates human immunodeficiency virus type-1 late gene expression. *J. Mol. Biol.* **241**, 193–207.
3. Daly, T. J., Doten, R. C., Rennert, P., Auer, M., Jaksche, H., Donner, A. *et al.* (1993). Biochemical characterization of binding of multiple HIV-1 Rev monomeric proteins to the Rev responsive element. *Biochemistry*, **32**, 10497–10505.
4. Daly, T. J., Cook, K. S., Gray, G. S., Maione, T. E. & Rusche, J. R. (1989). Specific binding of HIV-1 recombinant Rev protein to the Rev-responsive element *in vitro*. *Nature*, **342**, 816–819.
5. Malim, M. H., Bohnlein, S., Hauber, J. & Cullen, B. R. (1989). Functional dissection of the HIV-1 Rev trans-activator—derivation of a trans-dominant repressor of Rev function. *Cell*, **58**, 205–214.
6. Malim, M. H. & Cullen, B. R. (1991). HIV-1 structural gene expression requires the binding of multiple Rev monomers to the viral RRE: implications for HIV-1 latency. *Cell*, **65**, 241–248.
7. Cochrane, A. W., McNally, M. T. & Mouland, A. J. (2006). The retrovirus RNA trafficking granule: from birth to maturity. *Retrovirology*, **3**, 18.
8. Fang, J., Kubota, S., Yang, B., Zhou, N., Zhang, H., Godbout, R. & Pomerantz, R. J. (2004). A DEAD box protein facilitates HIV-1 replication as a cellular co-factor of Rev. *Virology*, **330**, 471–480.
9. Fang, J., Acheampong, E., Dave, R., Wang, F., Mukhtar, M. & Pomerantz, R. J. (2005). The RNA helicase DDX1 is involved in restricted HIV-1 Rev function in human astrocytes. *Virology*, **336**, 299–307.
10. Pyle, A. M. (2008). Translocation and unwinding mechanisms of RNA and DNA helicases. *Annu. Rev. Biophys.* **37**, 317–336.
11. Rocak, S. & Linder, P. (2004). DEAD-box proteins: the driving forces behind RNA metabolism. *Nat. Rev., Mol. Cell Biol.* **5**, 232–241.
12. Edgcomb, S. P., Carmel, A. B., Naji, S., Ambrus-Aikelin, G., Reyes, J. R., Saphire, A. C. S. *et al.* (2011). Submitted for publication.
13. Pond, S. J., Ridgeway, W. K., Robertson, R., Wang, J. & Millar, D. P. (2009). HIV-1 Rev protein assembles on viral RNA one molecule at a time. *Proc. Natl Acad. Sci. USA*, **106**, 1404–1408.
14. Yang, Q. & Jankowsky, E. (2005). ATP- and ADP-dependent modulation of RNA unwinding and strand annealing activities by the DEAD-box protein DED1. *Biochemistry*, **44**, 13591–13601.
15. Halls, C., Mohr, S., Del Campo, M., Yang, Q., Jankowsky, E. & Lambowitz, A. M. (2007). Involvement of DEAD-box proteins in group I and group II intron splicing. Biochemical characterization of Mss116p, ATP hydrolysis-dependent and -independent mechanisms,

and general RNA chaperone activity. *J. Mol. Biol.* **365**, 835–855.
16. Chamot, D., Colvin, K. R., Kujat-Choy, S. L. & Owttrim, G. W. (2005). RNA structural rearrangement via unwinding and annealing by the cyanobacterial RNA helicase, CrhR. *J. Biol. Chem.* **280**, 2036–2044.
17. Henn, A., Cao, W., Licciardello, N., Heitkamp, S. E., Hackney, D. D. & De La Cruz, E. M. (2010). Pathway of ATP utilization and duplex rRNA unwinding by the DEAD-box helicase, DbpA. *Proc. Natl Acad. Sci. USA*, **107**, 4046–4050.
18. Chen, Y., Potratz, J. P., Tijerina, P., Del Campo, M., Lambowitz, A. M. & Russell, R. (2008). DEAD-box proteins can completely separate an RNA duplex using a single ATP. *Proc. Natl Acad. Sci. USA*, **105**, 20203–20208.
19. Liu, F., Putnam, A. & Jankowsky, E. (2008). ATP hydrolysis is required for DEAD-box protein recycling but not for duplex unwinding. *Proc. Natl Acad. Sci. USA*, **105**, 20209–20214.
20. DiMattia, M. A., Watts, N. R., Stahl, S. J., Rader, C., Wingfield, P. T., Stuart, D. I. *et al.* (2010). Implications of the HIV-1 Rev dimer structure at 3.2 Å resolution for multimeric binding to the Rev response element. *Proc. Natl Acad. Sci. USA*, **107**, 5810–5814.
21. Edgcomb, S. P., Aschrafi, A., Kompfner, E., Williamson, J. R., Gerace, L. & Hennig, M. (2008). Protein structure and oligomerization are important for the formation of export-competent HIV-1 Rev–RRE complexes. *Protein. Sci.* **17**, 420–430.
22. Jankowsky, E. & Fairman, M. E. (2007). RNA helicases—one fold for many functions. *Curr. Opin. Struct. Biol.* **17**, 316–324.
23. Pljevaljcic, G., Robertson-Anderson, R. M. & Millar, D. P. (2011). Analysis of RNA folding and ribonucleoprotein assembly by single-molecule fluorescence spectroscopy. *Methods Mol. Biol.*, Humana Press. In press.